NeuroImage: Clinical 9 (2015) 223–232

Contents lists available at ScienceDirect

NeuroImage: Clinical

journal homepage: www.elsevier.com/locate/ynicl

Default mode network segregation and social deficits in autism spectrum disorder: Evidence from non-medicated children

DMN in children with ASD

Benjamin E. Yerys[a,b,c,d,*], Evan M. Gordon[e], Danielle N. Abrams[b,f], Theodore D. Satterthwaite[g], Rachel Weinblatt[c], Kathryn F. Jankowski[c,h], John Strang[c,d], Lauren Kenworthy[c,d], William D. Gaillard[d], Chandan J. Vaidya[d,h]

[a]Center for Autism Research, The Children's Hospital of Philadelphia, Philadelphia, PA 19104, USA
[b]Department of Psychiatry, Perelman School of Medicine, University of Pennsylvania, Philadelphia, PA 19104, USA
[c]Center for Autism Spectrum Disorders, Children's National Health System, USA
[d]Center for Neuroscience, Children's National Health System, Washington, DC, USA
[e]Neurology Department, Washington University School of Medicine, Washington, DC, USA
[f]Psychology Department, Georgia State University, Atlanta, GA, USA
[g]Brain Behavior Laboratory, Department of Psychiatry, Perelman School of Medicine, University of Pennsylvania, Philadelphia, PA 19104, USA
[h]Psychology Department, University of Oregon, Eugene, OR, USA

ARTICLE INFO

Article history:
Received 24 March 2015
Received in revised form 31 July 2015
Accepted 31 July 2015
Available online 18 August 2015

Keywords:
Default mode network
Autism spectrum disorders
Functional connectivity
Resting state

ABSTRACT

Functional pathology of the default mode network is posited to be central to social-cognitive impairment in autism spectrum disorders (ASD). Altered functional connectivity of the default mode network's midline core may be a potential endophenotype for social deficits in ASD. Generalizability from prior studies is limited by inclusion of medicated participants and by methods favoring restricted examination of network function. This study measured resting-state functional connectivity in 22 8–13 year-old non-medicated children with ASD and 22 typically developing controls using seed-based and network segregation functional connectivity methods. Relative to controls the ASD group showed both under- and over-functional connectivity within default mode and non-default mode regions, respectively. ASD symptoms correlated negatively with the connection strength of the default mode midline core—medial prefrontal cortex–posterior cingulate cortex. Network segregation analysis with the participation coefficient showed a higher area under the curve for the ASD group. Our findings demonstrate that the default mode network in ASD shows a pattern of poor segregation with both functional connectivity metrics. This study confirms the potential for the functional connection of the midline core as an endophenotype for social deficits. Poor segregation of the default mode network is consistent with an excitation/inhibition imbalance model of ASD.

1. Introduction

Humans have an incredible capacity to reflect upon their own or others' emotional states. The default mode network (DMN) is a large-scale brain network involved in processing one's own or others' emotional state (Buckner et al., 2008). Impairments in this type of mental reflection are part of the social-cognitive symptoms that define autism spectrum disorders (ASD; Castelli et al., 2002; Kana et al., 2014; Lombardo et al., 2010; Uddin et al., 2008). The DMN has been hypothesized as a candidate locus of pathology in ASD. This network includes the medial prefrontal cortex (MPFC), medial parietal regions (posterior cingulate cortex (PCC) and adjoining precuneus, and retrosplenial cortex), lateral parietal regions (angular gyrus (AG)), and temporal regions. In individuals with ASD, these regions show abnormal gray matter volume (Uddin et al., 2011), abnormal histopathology (Casanova et al., 2006; Oblak et al., 2011), and reduced activation during tasks that require reflecting on emotional states (theory-of-mind and self/other judgments; Castelli et al., 2002; Kana et al., 2014; Lombardo et al., 2010; Uddin et al., 2008). Further, deactivation of DMN regions accurately classified ASD from control subjects (Murdaugh et al., 2012). Together, these findings support DMN functional pathology as a contributor to social-cognitive impairments in ASD.

* Corresponding author at: Center for Autism Research, The Children's Hospital of Philadelphia, Ste 860, 3535 Market Street, Philadelphia, PA 19104, USA. Tel.: +1 267 426 1470; fax: +1 267 426 7590.
E-mail address: yerysb@email.chop.edu (B.E. Yerys).

http://dx.doi.org/10.1016/j.nicl.2015.07.018

Table 1
Summary table of all resting state default mode network studies in ASD.

Reference	Groups/demographics		Analysis	Group differences
	ASD	Control		
Kennedy and Courchesne (2008)	n = 12 (8)* Age *M* = 26.5 FSIQ *M* = 101.6	n = 13 Age *M* = 27.5 *M* = 105.6	Voxel-wise correlation based analysis from 3 *a priori* regions-of-interest (MPFC, PCC, left AG)	Reduced FC in MPFC and left AG for ASD vs. controls
Monk et al. (2009)	n = 12 (10,8,7) Age *M* = 26; VIQ *M* = 117 PIQ *M* = 119	n = 12 Age *M* = 27 VIQ *M* = 110 PIQ *M* = 118	Pairwise correlation with PCC as seed and correlated with 11 other DMN regions	1) Reduced FC in PCC-right SFG for ASD vs. controls 2) Increased FC in PCC-right TempL and PCC-right PHC for ASD vs. controls
Weng et al. (2010)	n = 16 (6) Age *M* = 15 VIQ *M* = 114 NVIQ *M* = 117	n = 14 Age *M* = 16 VIQ *M* = 113, NVIQ *M* = 106	Pairwise correlation with PCC as seed and correlated with 11 other DMN regions	Reduced FC from PCC to 9 of 11 DMN regions in ASD vs. controls: RSC, bilateral MPFC, bilateral SFG, bilateral TempP, bilateral PHC
Assaf et al. (2010)	n = 15 Age *M* = 15.7 FSIQ *M* = 113.3	n = 15 Age *M* = 17.1 FSIQ *M* = 117.1	Independent components analysis −3 DMN components were selected and compared for strength of each component/sub-DMN network between groups	Reduced FC in PrC (sub-network A) and MPFC (sub-network C) for ASD vs. controls
Wiggins et al. (2011)	n = 39 (17) Age *M* = 14.0 VIQ *M* = 108.2 NVIQ *M* = 111.54	n = 41 Age *M* = 15.3 VIQ *M* = 116.5 NVIQ *M* = 105.4	Used a self-organizing map to identify subject specific seed	Reduced FC from PCC to right superior frontal gyrus and right IPL in ASD vs. controls
von dem Hagen et al. (2013)	n = 17 (16) Age *M* = 30 FSIQ *M* = 116 VIQ *M* = 112 PIQ *M* = 117	n = 24 Age *M* = 25 FSIQ *M* = 118 VIQ *M* = 115 PIQ *M* = 117	Compared DMN from ICA components and voxel-wise correlation with MPFC, PCC, AG, aInsula, and amyg as seeds. Small volume corrected differences within 6 a priori seeds	1) ICA showed reduced FC in the MPFC for ASD vs. controls 2) Seed based analysis showed reduced FC from MPFC to TempL and to amyg
Lynch et al. (2013)	n = 20 Age *M* = 9.96 FSIQ *M* = 112.6	n = 19 Age *M* = 9.88 FSIQ *M* = 112.2	Voxel-wise correlation with 3 seeds from posterior midline DMN node (PCC, RSC, Prec)	1) Prec seed showed reduced FC in ASD to cuneus, right thalamus, and bilateral caudate 2) RSC seed showed increased FC in ASD to PHC, left pSTS, right pInsula, left TempP 3) PCC seed showed increased FC in ASD to PHC, ERc/PRc, aLTC, TempP
Eilam-Stock et al. (2014)	n = 17 (17) Age *M* = 26.1 FSIQ *M* = 110.3	n = 15 Age *M* = 27.1 FSIQ *M* = 112.6	Voxel-wise correlation with whole-brain from a PCC and an MPFC seed	1) Decreased FC in ASD group for Prec, MPFC/ACC, pInsula, STG, ITG, GR, IPL and LOG, 2) Increased FC in ASD group within the medial TempL
Jung et al. (2014)	n = 19 Age *M* = 25.3 FSIQ *M* = 109.7	n = 21 Age *M* = 24.8 FSIQ *M* = 109.5	Voxel-wise correlation with whole-brain from a PCC and MPFC seed	1) MPFC seed showed decreased FC in ASD group for primary motor and sensory cortices and MFG 2) PCC seed showed decreased FC in ASD group for MPFC
Doyle-Thomas et al. (2015)	n = 58 (58) Age *M* = 12.5 FSIQ *M* = 98.7	n = 37 Age *M* = 12.7 FSIQ *M* = 116.9	Voxel-wise correlation with whole-brain from an "eroded" Left PCC and Right PCC seed; Secondary analysis of pairwise correlation with PCC seeds to 8 other DMN regions	1) PCC seeds showed decreased FC in ASD to left MPFC, bilateral AG, right ITG (whole--brain) 2) PCC–MPFC connection was reduced in ASD with pairwise correlations 3) PCC–MPFC functional connectivity decreased with age in ASD group, but increased with age in control group 4) Slopes differed between groups on correlation between DMN connections and measure of empathy. Better performance and weaker correlations for ASD (left PCC-right MPFC, right PCC to bilateral Prec, right MPFC). Opposite pattern for right PCC to right MTG

ACC = anterior cingulate cortex; AG = angular gyrus; aInsula = anterior insula; LTC = anterolateral temporal cortex; amyg = amygdala; ASD = autism spectrum disorder; DMN = default mode network; ERc = entorhinal cortex; FC = functional connectivity; GR = gyrus rectus; IPL = intra-parietal lobule; ITG = inferior temporal gyrus; LOG = lateral occipital gyrus; MPFC = medial prefrontal cortex; MTG = medial temporal gyrus; NVIQ = nonverbal IQ; PCC = posterior cingulate cortex; PHC = parahippocampal gyrus; pInsula = posterior insula; PRc = perirhinal cortex; Prec = precuneus; pSTS = posterior superior temporal sulcus; RSC = retrosplenial cortex; SFG = superior frontal gyrus; STG = superior temporal gyrus; TempL = temporal lobe; TempP = temporal pole; VIQ = verbal IQ.

* Number in parentheses is the portion of the sample that is included in medication free analysis. Multiple numbers indicates that analyses were run for individual medications (run analyses without those taking stimulants or those taking SSRIs). Studies without a number in parentheses indicates no such analyses were conducted.

Functional pathology of the DMN in ASD is also apparent in functional connectivity analyses (temporal correlations between regions). Functional connectivity can be measured in task-evoked and in task-free/resting state (Smith et al., 2009) or during sleep (Fukunaga et al., 2006). Resting state functional connectivity is posited to at least partly reflect the statistical history of interactions between brain regions (Dosenbach et al., 2007). In youth and adult ASD groups, task-evoked functional connectivity of DMN regions is reduced relative to controls during theory-of-mind (Mason et al., 2008), social exclusion (Bolling et al., 2011), and face processing (Kleinhans et al., 2008) tasks. Similarly, resting-state studies show that functional connectivity of the DMN is altered in ASD. The midline core, the PCC–MPFC connection, is consistently reduced in adults and adolescents with ASD relative to controls (Assaf et al., 2010; Doyle-Thomas et al., 2015; Jung et al., 2014; Kennedy and

Courchesne, 2008; Monk et al., 2009; Ray et al., 2014; Rudie et al., 2012a; von dem Hagen et al., 2013; Weng et al., 2010; Wiggins et al., 2011) and predicts social impairment in ASD across the age span (Assaf et al., 2010; Doyle-Thomas et al., 2015; Eilam-Stock et al., 2014; Jung et al., 2014; Monk et al., 2009; see Table 1). However, non-midline DMN regions like the AG (Doyle-Thomas et al., 2015; Kennedy and Courchesne, 2008; Lynch et al., 2013; Monk et al., 2009; Weng et al., 2010) or amygdala/temporal regions (Lynch et al., 2013; von dem Hagen et al., 2013) show mixed results of over- and under-connectivity to the PCC or MPFC in both youth and adults with ASD. The convergence of findings from both task-evoked and task-free functional connectivity paradigms, which both indicate atypical midline DMN function in ASD, has raised this circuit's potential as an endophenotype for ASD.

1.1. Limitations in connectivity methods

However, gaps remain in our understanding of the DMN's functional connectivity in ASD, which limit its potential as an endophenotype. Most studies have used a region-to-region correlation or seed-region-to-whole-brain regression approach that has yielded a consistent pattern of lower DMN functional connectivity in youth and adults with ASD (Cherkassky et al., 2006; Kennedy and Courchesne, 2008; Monk et al., 2009; von dem Hagen et al., 2013; Weng et al., 2010; Assaf et al., 2010; Wiggins et al., 2011; Eilam-Stock et al., 2014; Jung et al., 2014; Doyle-Thomas et al., 2015), but provides a limited field of view (von dem Hagen et al., 2013). Region-to-region analyses only assess functional connectivity among the selected regions. Seed-region-to-whole-brain regression analyses provide full-brain coverage but only from the selected seeds, and most prior studies did not use seeds from all DMN regions (Doyle-Thomas et al., 2015; Jung et al., 2014; Lynch et al., 2013; Monk et al., 2009; Weng et al., 2010). Using a single (or subset) of seeds for regression analyses may skew the interpretation of an entire network. Characteristics of cross-network relationships, such as the degree of network segregation or integration, have proven useful in understanding normative developmental changes during childhood (Fair et al., 2007; Satterthwaite et al., 2013b), individual differences in behavioral traits (e.g. anxiety, empathy, socialness) (see review Vaidya and Gordon, 2013), and altered neural function in psychiatric and neurological disorders with altered network segregation (Bassett and Bullmore, 2009).

Graph theory metrics are a newer approach to quantifying the segregation and integration of a network (Bullmore and Sporns, 2009; Rubinov and Sporns, 2010). Two studies utilized graph theory in characterizing the DMN (and other networks) in youth with ASD (Ray et al., 2014; Rudie et al., 2012a). Both studies converged with seed based findings to demonstrate generally reduced magnitude of connections within the DMN, and increased magnitude/number of connections between DMN and non-DMN regions.

Employing a traditional seed-based approach and a graph theory approach to the same data set enriches the present study's capacity to inform the literature. The present study will be able to integrate these two forms of functional connectivity analyses in the same participants to demonstrate that the two approaches converge upon the same result in the same set of children.

1.2. Interference of psychotropic medication

Psychotropic medication likely influenced past DMN studies in ASD. For example, SSRIs reduced MPFC functional connectivity to medial temporal regions in healthy adults (McCabe and Mishor, 2011). Treatment with atypical antipsychotics in schizophrenia (Sambataro et al., 2010), and stimulants or SNRIs in ADHD (Marquand et al., 2011; Wilson et al., 2013) have increased PCC–MPFC functional connectivity. Almost all youth and adult ASD groups in past DMN studies were imaged while taking selective serotonin reuptake inhibitors (SSRIs) (Assaf et al., 2010; Lynch et al., 2013; Monk et al., 2009; von dem Hagen et al., 2013; Weng et al., 2010; Wiggins et al., 2011), neuroleptics (Assaf et al., 2010; Lynch et al., 2013; Monk et al., 2009; Weng et al., 2010; Wiggins et al., 2011), antipsychotics (Assaf et al., 2010; Monk et al., 2009; Weng et al., 2010; Wiggins et al., 2011), stimulants (Assaf et al., 2010; Lynch et al., 2013; Monk et al., 2009; Weng et al., 2010; Wiggins et al., 2011), alpha-2A agonists (Lynch et al., 2013; Monk et al., 2009), selective norepinephrine reuptake inhibitors (SNRIs) (Monk et al., 2009), and anti-convulsants (Assaf et al., 2010; Weng et al., 2010). Some of these studies reported secondary analyses showing that medications did not influence group differences in the DMN, but the sample sizes of most of these studies were too small to be definitive (<10) and likely too small to confirm relationships with symptoms in youth and adults (Assaf et al., 2010; Kennedy and Courchesne, 2008; Lynch et al., 2013; Monk et al., 2009; Weng et al., 2010). Several studies had larger samples of medication free youth (Doyle-Thomas et al., 2015; Wiggins et al., 2011), and adults (Eilam-Stock et al., 2014; von dem Hagen et al., 2013) with ASD. One, which examined a large sample of non-medicated youth with ASD did observe reduced PCC–MPFC functional connectivity in children with ASD, and PCC–MPFC connectivity strength correlated with a measure of empathy (Doyle-Thomas et al., 2015). However, this study recruited a wide age-range of 6–17 years, and the DMN is known to change with age (Fair et al., 2007; Satterthwaite et al., 2013b). Thus, to confirm the DMN as an endophenotype of ASD this finding requires additional, independent replication in which a measure of ASD symptoms is used and the potential influence of age is minimized.

1.3. Age and head motion confounds

In most prior studies, participants' age was not tightly controlled. The largest pediatric study of children with ASD observed reduced PCC–MPFC functional connectivity in a sample ranging from early childhood to emerging adulthood (6–17 years) (Doyle-Thomas et al., 2015), but a study restricted to 9–13 year-olds did not observe reduced PCC–MPFC functional connectivity (Lynch et al., 2013). This finding may be related to developmental changes in PCC–MPFC functional connectivity during that age period (Gordon et al., 2011; Supekar et al., 2010), medication status, or a true non-difference. Thus, a study with a narrower age range may help to sort out the potential role of development in these two discrepant findings.

Small amounts of head motion biases measurement towards reduced functional connectivity between distant regions such as frontal and posterior cortices (Power et al., 2012; Satterthwaite et al., 2013b; Van Dijk et al., 2012). ASD groups often move more than controls (Yerys et al., 2009), which may result in spurious lower PCC–MPFC functional connectivity in ASD (Deen and Pelphrey, 2012). To assess the potential of the DMN as an endophenotype of ASD it is important to examine within and cross-network functional connectivity in a restricted age range of children while controlling for potential confounds associated with medication usage excessive head motion.

1.4. Present study

We evaluated the DMN resting state functional connectivity with two complementary approaches. We first used a seed-based analysis approach with six canonical DMN regions (Van Dijk et al., 2010). We then used a network analysis approach with a graph theory metric (i.e., participation coefficient, the ratio of within and cross-network functional connectivity) (Bullmore and Sporns, 2009; Rubinov and Sporns, 2010). The seed-based analysis identifies the most severely altered functional connectivity patterns for each DMN region—connections surviving multiple comparisons corrections—and facilitates cross-study comparison. The network analysis is complementary,

because it aggregates all of the individual DMN regions' functional connectivity into a single DMN score that quantifies within-network connectivity (segregation) and cross-network connectivity (integration). We imaged 8–13 year-old non-medicated children with ASD and typically developing controls, using established procedures to minimize head motion artifacts (Satterthwaite et al., 2013a). With seed-based analyses, we predicted that we would observe reduced functional connectivity of the MPFC–PCC connection in the ASD group, and individual differences in MPFC–PCC connectivity strength would correlate negatively with the severity of social-cognitive impairments within the ASD group (Assaf et al., 2010; Doyle-Thomas et al., 2015; Jung et al., 2014; Monk et al., 2009). Past studies have not examined the functional connectivity of remaining DMN nodes in children with ASD; therefore we lacked bases for making predictions for those regions. At the network level, prior mixed findings within the DMN coupled with recent knowledge of over-connectivity when motion is well-controlled in children with ASD (Supekar et al., 2013) lead us to predict a disruption in the segregation of the DMN with other large-scale networks. Therefore, we predicted the ASD group's DMN participation coefficient would be higher than controls, representing reduced DMN segregation from other networks.

2. Method

2.1. Participants

Twenty-two non-medicated children with ASD and 22 typically developing control (TDC) children matched on age, IQ, and sex ratio were included in the study (see Table 2). Five additional children (3 ASD) were excluded due to excessive motion. All children had Full-Scale IQ > 80, and no history of seizure disorder. All ASD participants were not on psychotropic medication while completing the scan, except for one participant who was prescribed a stimulant. This one child was medication free for 24 h prior to scanning, and excluding this child did not change the results. These children were part of a prior study's cohort (Supekar et al., 2013). ASD diagnoses were made using DSM-IV-TR criteria and confirmed with the Autism Diagnostic Observation Schedule (ADOS) (Lord et al., 2000) and Autism Diagnostic Interview—Revised (Lord et al., 1994). TDCs were screened for developmental delays, learning, psychiatric, and neurological disorders through a phone interview, and T-scores below the threshold of clinical score (T-score < 65) for all childhood psychiatric disorders on the Child and Adolescent Symptom Inventory (Gadow and Sprafkin, 2010).

Table 2
Participant characteristics.

	TDC (n = 22)	ASD (n = 22)	*p*-Value
Chronological age (years)			
M (SD)	11.37 (1.56)	11.41 (1.51)	0.93
Range	8.50–13.58	8.42–13.83	–
Full Scale IQ			
M (SD)	117.64 (10.67)	112.68 (13.66)	0.19
Range	104–136	83–138	–
Sex-ratio (M:F)	18:4	18:4	1.00
ADI-R			
Reciprocal social interaction	–	20.05 (5.37)	
Communication	–	15.95 (4.49)	
Repetitive behaviors	–	4.86 (1.98)	
ADOS			
Social + communication *M* (SD)	–	11.00 (3.19)	
Severity score *M* (SD)	–	6.59 (1.74)	

ASD = autism spectrum disorder; TDC = typically developing control.

The Institutional Review Boards of the participating institutions approved the research protocol, consent was obtained from parents and assent from participants in accordance with the Declaration of Helsinki, and participants received monetary compensation.

2.2. Imaging procedure

Functional images were acquired on a 3 T Siemens Trio scanner using a *T2**-sensitive gradient echo pulse sequence: 154 whole-brain volumes, 43 slices, TR/TE/FOV/flip angle/voxel size = 2000/31 ms/256 × 256 mm/90°/3 mm isotropic. Seven children (5 TDC) received an alternate sequence: 150 whole-brain volumes, 37 slices, TR/TE/FOV/flip angle/voxel size = 2000/30 ms/192 × 192 mm/90°/3 mm isotropic. A high-resolution T1-weighted image for co-registration of the functional images was acquired with Siemens MPRAGE sequence: TR/TE/TI/FOV/slices/flip angle = 1900/2.52/900 ms/256 × 256 mm/176 1 mm^3 slices/90°. Participants were instructed to keep their eyes open and lie still while the monitor displayed a black screen. Resting state data were collected in the middle of a sequence of fMRI runs for the seven children receiving an alternate sequence, but first for the remaining children; all results remained significant after excluding those seven children.

2.3. Subject level time series processing

All preprocessing was completed in FSL (Smith et al., 2004) or using in-house scripts (Satterthwaite et al., 2013a). Functional images were brain extracted, the first four volumes were removed to allow for BOLD signal stabilization, and then all images were slice-time corrected, motion corrected to the median volume, spatially smoothed (7 mm FWHM), grand mean scaled with mean-based intensity normalization, and co-registered with boundary-based registration. Each subject's time series was then normalized into the Montreal Neurological Institute standard anatomical space (2 mm template) using the deformable registration via attribute matching and mutual saliency software (Ou et al., 2011). Prior to motion artifact correction, we compared the mean relative displacement between groups generated by FSL's MCFLIRT, which is the mean value of the root mean square relative to the previous volume. Groups were matched (ASD M = 0.09, SD = 0.04; TDC M = 0.09, SD = 0.04; p = 0.78).

We minimized head motion artifacts by using a validated procedure that regresses out common motion and physiological noise with a 36-parameter model from the time course of each voxel (Satterthwaite et al., 2013a). The confound regression model included 24 parameters related to motion artifact: six realignment parameters, the temporal derivative of each realignment parameter, and inclusion of the quadratic term for the previous 12 parameters. A total of 12 parameters related to physiological noise were estimated from the mean global signal regression, white matter (WM), and cerebrospinal fluid (CSF); their temporal derivatives; and the quadratic terms for the previous 6 parameters. WM and CSF were defined on a subject-specific basis through segmentation of the T1-weighted image using Deformable Registration via Attribute Matching and Mutual-Saliency Weighting software (Ou et al., 2011) and other internal software (Multiplicative Intrinsic Component Optimization). Prior to regression, we band-pass filtered the functional time series, the seed, and the confound regressors to retain frequencies between 0.01 and 0.08 Hz. Seed and confound regressors were filtered to prevent a mismatch in the frequency domain and to allow the best fit between the confound parameters and the retained signal frequencies (Hallquist et al., 2013).

2.4. Seed-based analysis

Four millimeter radius spheres for six DMN regions of interest (ROIs) were generated in MARSBAR (Brett et al., 2002), centered around

coordinates taken from a large *N* study that established the reliability of DMN functional connectivity (Van Dijk et al., 2010). The DMN ROIs included the PCC (MNI coordinates: 0, −53, 6), MPFC (0, 52, −6), left and right AG (−48, −62, 36; 46, −62, 32), and left and right hippocampus (HC; −24, −22, −20; 24, −22, −20; see Fig. 1). For each participant, a multiple regression was conducted with the extracted time series for each seed ROI entered as the covariate of interest, and the 36 confound signals entered as covariates of no interest. This resulting map was transformed to a z-stat map with Fisher's *r-to-z* transformation, and then entered into group-level random effects analysis, with age, sex, Full-Scale IQ, and root mean squared volume-to-volume displacement of all voxels as covariates of no interest. Voxel-wise and cluster-extent thresholds of $Z > 2.6$ and $p < 0.05$ were used.

To replicate prior research within the ASD group, we conducted post-hoc correlations between the ADOS calibrated severity score (Gotham et al., 2009) and Fisher's *r-to-z* values for connections that differed between groups. Prior studies showed a correlation between the MPFC–PCC connection and ADOS scores in adults and children (Assaf et al., 2010; Doyle-Thomas et al., 2015; Jung et al., 2014; Monk et al., 2009). Because of the existing evidence supporting an a priori hypothesis that the MPFC–PCC would correlate with ASD symptoms, we did not include it in our multiple comparisons correction; for all other correlations between ADOS scores and functional connections we used a False Discovery Rate of $q < 0.05$ to correct for multiple comparisons (Benjamini and Hochberg, 1995).

2.5. Network segregation analysis

We extracted time series data from a 264-ROI parcellation scheme, which was previously mapped to 14 functional networks with an independent sample (Power et al., 2011). The functional networks include the DMN, visual, auditory, salience, cingulo-opercular, frontal–parietal, memory retrieval, cerebellum, sensory-somatomotor-hand, sensory-somatomotor-mouth, subcortical, ventral attention, dorsal attention, and uncertain. The uncertain network includes ROIs that do not correlate with any functional network. We created a 264 × 264 functional connectivity matrix of pairwise Pearson's correlations. We converted correlations into a sparse and binary form (Power et al., 2011), and then calculated the participation coefficient of each ROI across a range of binarization thresholds to characterize the properties of the DMN (Power et al., 2011; Rubinov and Sporns, 2010). This approach minimizes potential spurious connections. The participation coefficient is a summary network topology measure that quantifies how connected a defined ROI is to other ROIs within and across networks (Rubinov and Sporns, 2010). A higher participation coefficient indicates more cross-network connections, denoting network integration. In contrast, a lower participation coefficient indicates more within-network connections, denoting segregation. We created a mean DMN participation coefficient by taking the mean of all 58 ROIs labeled as DMN regions within the established community structure of this ROI set (Power et al., 2011). We plotted the participation coefficient for each individual's DMN using a range of binarization thresholds ranging from r = .1 to r = .7, and then calculated the DMN's Area Under the Curve (AUC). Higher AUC scores correspond to greater network integration across all thresholds, and lower scores correspond to greater segregation. Group differences in AUC were compared in an analysis of covariance where age, sex, Full-Scale IQ, and root mean square were entered as covariates. For all analyses, we examined functional connectivity within a mask that included voxels present in every participant's scan. This led to partial cerebellum coverage, and included the following cerebellum ROIs from the 264-parcellation scheme: (−18, −76, −24); (−16, −65, −20), (−32, −55, −25); and (22, −58, −23). Group differences are interpreted within the 14 network community structure (Power et al., 2011). In one seed-based analysis a cluster emerged in the nucleus accumbens which is not represented in Power et al. (2011) a priori community structure; therefore, we interpreted this finding within the broader literature which points to this region as highly relevant for processing reward signals (Knutson et al., 2000; O'Doherty, 2004). The inclusion of the reward network in the seed-based analysis brings the total number of potential networks to 15, while the graph theory analysis only included the 14 network community structure.

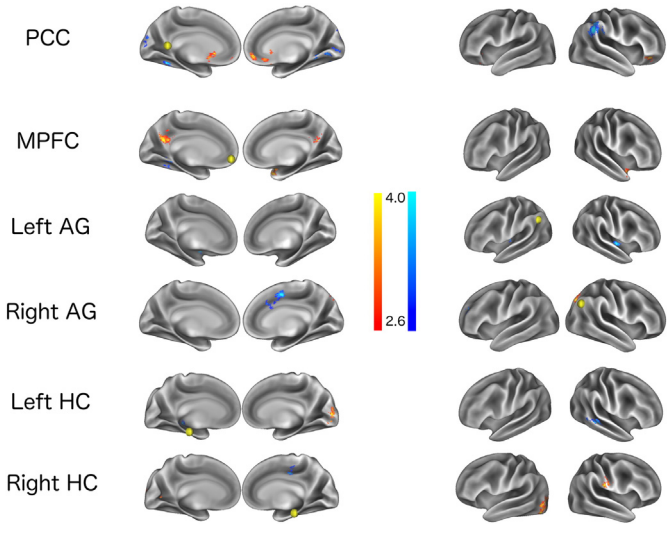

Fig. 1. Two-sample *t*-tests comparing the functional connectivity maps of the ASD and TDC groups by each seed ROI. Yellow spheres on the medial or lateral surface represent the seeds. Spheres are larger than 4 mm for visualization purposes. The TDC > ASD comparison is shown in the orange-yellow palette, and the ASD > TDC comparison is shown in the blue-light blue palette. All differences survive a voxel threshold of $Z > 2.6$ and cluster corrected at $p < 0.05$. The group difference of lower right AG-frontal pole cluster in ASD is not visible in this figure, but can be seen in Fig. S3.

3. Results

3.1. Seed-based analysis

3.1.1. Group differences from DMN seeds to DMN regions.

Compared to controls, the ASD group showed reduced functional connectivity from the PCC seed to a region in MPFC, and from the MPFC seed to a region in the PCC. The ASD group also had lower functional connectivity between the MPFC seed and the right temporal pole, as well as between the right AG seed and a left frontal pole region (see Fig. 1 and Table 3). See the SI for within group DMN maps. We further re-analyzed this data with 6 mm radius sphere ROIs. This secondary re-analysis demonstrated that the pattern of results was not changed by ROI size (see SI).

3.1.2. Group differences from DMN seeds to the rest of the brain.

Compared to the TDC group, the ASD group showed reduced functional connectivity between the DMN ROIs and several regions involved in primary sensory networks (Visual, Somatosensory, Motor), higher-level association networks (Fronto-Parietal), as well as the Subcortical and Reward networks. The DMN ROIs also had increased functional connectivity with several regions in primary sensory networks (Visual, Somatosensory, Motor) and higher-level association networks (Salience and Ventral Attention). See Table 3 for detailed descriptions of group differences for each seed.

3.1.3. Correlation with social symptoms

There was a significant negative correlation between the MPFC seed–PCC cluster and ASD symptoms, $r = -0.51$, $p = 0.01$. See Fig. 2. The correlation between the PCC seed–MPFC cluster and ASD symptoms

Table 3
Group differences in FC of default mode network regions with seeds.

	Region	BA	Peak MNI coordinate			Voxels	Peak *z*-score
			X	Y	Z		
PCC							
ASD > TDC	Supramarginal gyrus	40	54	−40	32	725	4.23
	Lingual gyrus	19	18	−48	−10	374	4.23
	Occipital pole	17	−8	−92	8	361	3.76
	Occipital pole	19	18	−92	26	282	3.66
	Fusiform gyrus	37	−30	−48	−14	149	4.24
	Fusiform gyrus	37	38	−66	−20	143	3.83
TDC > ASD	Nucleus accumbens	–	−6	20	−4	730	4.55
	Medial prefrontal cortex	10	10	48	−8	279	4.23
	Orbitofrontal cortex	47	32	38	−10	212	4.27
	Cerebellum	–	0	−48	−30	125	4.05
MPFC							
ASD > TDC	Cerebellum	–	−26	−50	−24	279	3.97
TDC > ASD	Precuneus/PCC	31/23	−2	−58	24	535	4.55
	Temporal pole	38	36	14	−26	525	4.47
	Pallidum	–	16	−8	−2	162	5.10
Left AG							
ASD > TDC	Pallidum	–	−16	−2	−2	342	3.24
	Putamen	–	−26	−14	8	122	3.82
	Insula	13	40	−16	−2	90	3.59
Right AG							
ASD > TDC	Frontal pole	10	−28	48	28	243	4.41
	Mid-cingulate/SMA	6	8	−2	48	241	5.04
TDC > ASD	Lateral occipital	7	28	−76	40	269	4.54
	Frontal pole	10	20	38	−6	114	3.58
Left HC							
ASD > TDC	pSTG	21	48	−36	0	239	3.60
	Cerebellum	–	−2	−44	−8	148	3.87
	Pallidum	–	−22	−8	0	138	3.54
	Thalamus	–	−14	−32	2	106	4.1
	Cerebellum	–	42	−64	−26	104	3.57
TDC > ASD	Lingual gyrus	18	4	−90	−10	114	3.56
Right HC							
ASD > TDC	Middle cingulate	31	10	−22	42	112	3.95
TDC > ASD	Lateral occipital	19	−42	−82	10	626	5.34
	Postcentral gyrus	1	68	−14	30	204	4.1
	Occipital pole	18	0	−94	28	135	3.9

BA = Brodmann's area; PCC = posterior cingulate cortex; pSTG = posterior superior temporal gyrus; SMA = supplementary motor area.

was in the same direction, but non-significant, $r = -0.34$, $p = 0.13$. No other correlations survived FDR correction.

3.2. Network segregation analyses

Mean AUC was significantly lower in the TDC group (M = 28.95; SD = 2.02) than the ASD group (M = 30.14, SD = 1.97), z = 1.99, $p < 0.05$ (see Fig. 3), indicating poorer DMN segregation in the ASD group. We explored whether this effect was driven by reduced segregation between the DMN and specific networks by comparing the raw (weighted) mean participation coefficient for each network across groups. The participation coefficient for the DMN–Salience network was higher in ASD than the TDC group, $F(1,38) = 5.48$, $p = 0.02$ (see SI for details).

4. Discussion

Comprehensive examination of DMN functional connectivity in non-medicated children with ASD yielded three main findings: First, as hypothesized, the connections between the midline DMN core regions, MPFC and PCC, were reduced in the ASD group relative to controls. Within the ASD group, lower connectivity in this connection PCC–MPFC strength correlated with poorer social function. Second, seed-based analyses showed a mixed pattern of under- and/or over-connectivity in ASD children between multiple DMN nodes and those of other networks including Visual, Subcortical, Motor, Somatosensory, Salience, Ventral Attention, and Reward. These findings were evident even when manipulating the size of the seed ROI. Third, network analyses revealed that the DMN interacted with other networks to a greater extent in the ASD group, as indicated by a higher participation coefficient.

The present findings should be interpreted in light of the following methodological considerations. First, seed/ROI specifications differ between our study and prior research (Assaf et al., 2010; Di Martino et al., 2014; Doyle-Thomas et al., 2015; Jung et al., 2014; Kennedy and Courchesne, 2008; Lynch et al., 2013; Monk et al., 2009; Weng et al., 2010); however, our ability to replicate differences in PCC–MPFC connectivity, as well as the relationship to ASD symptoms lessens concern about this difference. We also elected to use an independent, validated a priori community for our graph theory analyses rather than deriving community structures from our own sample. There is no agreement about which community structure is best, and implementation of other parcellation schemes may have yielded different results; however we selected a community structure that was optimized for measuring intrinsic connectivity networks in resting state data. We also opted for

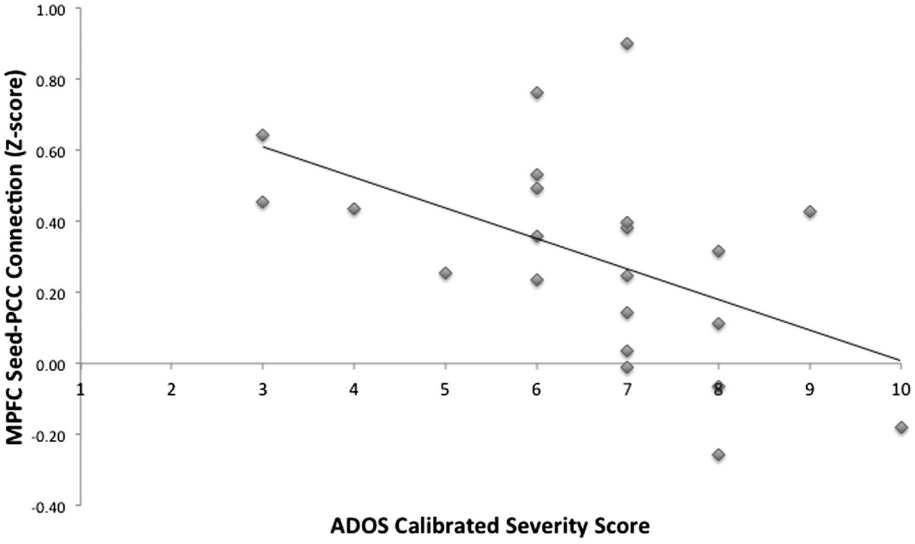

Fig. 2. This scatterplot shows the significant negative correlation between functional connectivity of the MPFC seed to a cluster in PCC (y-axis) and the Calibrated Severity Score from the Autism Diagnostic Observation Schedule (ADOS).

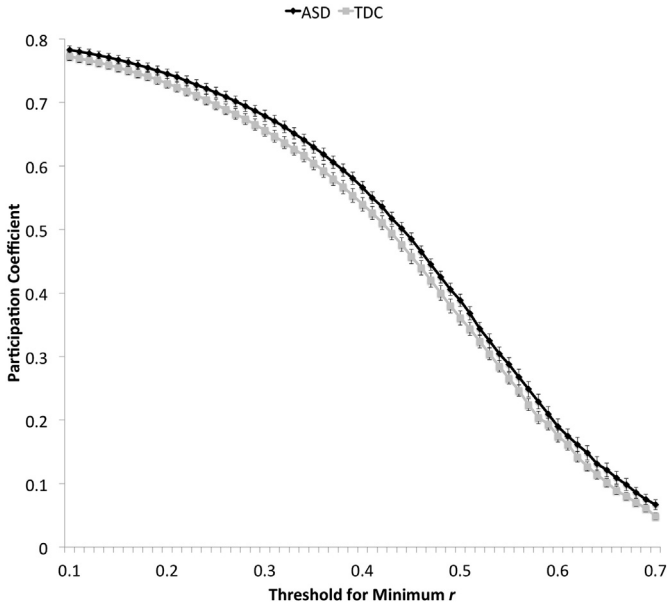

Fig. 3. Network analysis: the AUC plot for each group's participation coefficient (y-axis) across the range of minimum thresholds (x-axis).

an independent community, as establishing a community from our own TDC group would likely bias our results towards greater group differences because the TDC group is a perfect match to the community structure and the ASD group is not. Building a combined community structure would complicate interpretation, as this would not represent normative network architecture.

The second important methodological decision was that global signal regression (GSR) was employed in this study. GSR is the single most effective processing step for removing motion-related artifact in functional connectivity data (Power et al., 2014; Satterthwaite et al., 2013b), which is critically important when comparing groups likely to demonstrate differing degrees of motion, as in this study. However, we recognize that this procedure introduces a substantial negative bias in connectivity values (Fox et al., 2009), which can make it difficult to interpret observed negative connectivity strengths. Accordingly, we interpret all results from the present study in relative terms, e.g. as reflecting differences in the level of seed-to-region or network integration between the groups, rather than in absolute terms, e.g. as two regions or networks being more vs. less negatively connected in the groups.

Third, our ASD sample's cognitive ability was in the High Average range, which facilitates cross-study comparison, but limits generalization to those with intellectual disability. In addition, many of the children in our ASD sample may have received psychotropic medication in their lifetime and the long-term effects on functional connectivity cannot be quantified in the present study. However, we controlled for active psychotropic medication use on functional connectivity of the DMN.

Fourth, while we controlled for age, sex, and IQ, which are known to affect DMN functional connectivity in adolescents with ASD (Wiggins et al., 2011) and typical development (Satterthwaite et al., 2014); we did not match participants on puberty stages, which may have contributed to group differences.

4.1. The DMN midline core

Our study clarifies the nature of the DMN midline connection (PCC–MPFC) in ASD. First, consistent with most prior studies in ASD, functional connectivity of the PCC–MPFC was reduced in ASD. Importantly, this result was found in the present study after controlling for active psychotropic medication treatment and head motion, which is a critique of prior studies (Deen and Pelphrey, 2012). There is only one study to date that has examined a large non-medicated group of children with ASD (Doyle-Thomas et al., 2015), whereas other studies of youth and adults examined small non-medicated subsets (<10) (Assaf et al., 2010; Kennedy and Courchesne, 2008; Lynch et al., 2013; Monk et al., 2009; Weng et al., 2010). The prior large pediatric sample and the present study of non-medicated children suggest that medication effects do not drive reduced within-DMN functional connectivity in ASD. Furthermore, unlike past studies, we employed rigorous controls for head motion which, when uncontrolled, may bias functional connectivity estimates towards a pattern predicted by theoretical models of ASD—higher local functional connectivity and lower long-range functional connectivity (Deen and Pelphrey, 2012). Controlling for medication and head motion bolster confidence in the now well-replicated observation of weaker PCC–MPFC functional connectivity in youth and adults with ASD, as well as its negative correlation with ASD symptom severity (Assaf et al., 2010; Eilam-Stock et al., 2014; Jung et al., 2014; Monk et al., 2009). While only the MPFC seed yielded a significant relationship with ASD social symptoms, the PCC seed to MPFC cluster yielded a relationship of a medium effect (Cohen, 1988), which may have been underpowered to reach significance. We used the calibrated severity score rather than raw ADOS scores, which is a superior metric of symptom severity because of its independence from chronological age and verbal IQ (Gotham et al., 2009).

Our DMN midline functional connectivity findings converge with prior evidence of altered midline functional connectivity in ASD youth and adults (Cherkassky et al., 2006; Doyle-Thomas et al., 2015; Eilam-Stock et al., 2014; Jung et al., 2014; Monk et al., 2009; Weng et al., 2010), as well as atypical structural findings (Ameis et al., 2013; Cauda et al., 2011; Duerden et al., 2012; Ikuta et al., 2014; Jiao et al., 2010; Oblak et al., 2010, 2011; Rojas et al., 2006; Shukla et al., 2011; Uddin et al., 2011; Waiter et al., 2004) and task-evoked functional connectivity findings (Bolling et al., 2011; Kleinhans et al., 2008; Mason et al., 2008). The present study also converges with a recent, large multi-site resting state study that showed reduced functional connectivity between the PCC and MPFC in non-medicated children with ASD (Doyle-Thomas et al., 2015). However, these two studies differ from a third study of children with ASD that examined functional connectivity of the DMN with two distinct ROIs that separated the PCC and retrosplenial cortex based on anatomical boundaries (Lynch et al., 2013). This anatomically based study did not observe reduced PCC–MPFC functional connectivity, but instead observed increased functional connectivity with medial temporal and insula regions, which predicted social symptoms. The differing results of this study may relate to the inclusion of children taking psychotropic medication, differences in ROI placement, or regression of white matter and cerebro-spinal fluid signal in addition to global signal. We now know that these differences in method can contribute to discrepant findings across studies (Nair et al., 2014).

Our results augment the potential of PCC–MPFC functional connectivity as an endophenotype for social communication impairments in ASD. Considering criteria listed by Castellanos and Tannock (2002), it is a brain-based quantitative trait affiliated with the liability of ASD. The final criterion is heritability, and there is initial evidence that siblings of individuals with ASD show altered deactivation of the MPFC during mentalizing tasks (Murdaugh et al., 2012). Future research in this vein should focus on the clear demonstration of heritability within 1st degree family members using resting state data, tracking PCC–MPFC functional connectivity across development in ASD to examine its potential to predict long-term outcomes, and testing whether DMN functional connectivity changes with behavioral or pharmacological treatment.

4.2. DMN functional connectivity with other networks

Both statistical approaches used in this study suggest poor segregation of the DMN in ASD. The two approaches differ in their

measurement of functional connections. The seed-based approach examined relationships between the seed and every voxel in the brain, and so every possible connection difference is probed in the analysis. The network approach examined connections between ROIs that represented all networks within an established architecture, and this provides a context of how the DMN interacts as a whole with other large-scale networks. These different functional connectivity approaches converged to reveal atypical interactions between the DMN and other networks in ASD compared to controls.

The seed-based results demonstrated a mixed pattern of over- and under-connectivity for the DMN (i.e., the ASD group's DMN showed increased and decreased functional connectivity with regions in Visual, Motor, Somatosensory, Subcortical, Cerebellum, Salience, and Ventral Attention networks). This pattern converges with general conclusions drawn across functional connectivity studies of ASD, which have shown both increased and decreased functional connectivity across higher association and sensory networks (Müller et al., 2011). At a minimum, these results support reduced network segregation of the DMN in ASD. Our findings of reduced DMN segregation in ASD relative to controls converges with prior studies in youth with ASD (Ray et al., 2014; Rudie et al., 2012a,b; Shih et al., 2011). In two studies Rudie et al. (2012a,b) demonstrated decreased segregation in youth with ASD in the functional and structural connectivity of the DMN, visual, and sensorimotor, and social communication networks. Similarly, Ray et al. (2014) demonstrated that the magnitude of connections within highly connected or "rich-club" regions (MPFC and PCC) is smaller in children with ASD than controls. Shih et al. (2011) demonstrated that youth with ASD exhibited decreased segregation of the superior temporal sulcus with a social communication network that included DMN regions. By one view of network interaction, the DMN's putative role of internal prospective and reflective processing (Buckner et al., 2008; Raichle et al., 2001; Zhang and Raichle, 2010) is facilitated by its interaction with the Salience network, which directs toggling between intra-person (i.e., DMN) and extra-person (attributed to Fronto-Parietal or Visual networks) processing (Seeley et al., 2007; Uddin et al., 2014). We speculate that our secondary analysis revealing atypical DMN and Salience network interactions in the ASD group relate to a new hypothesis that altered DMN–Salience interactions reflect impaired toggling across brain states (Uddin et al., 2014).

We observed greater DMN interaction with networks responsible for signaling (Salience), processing (Visual, Sensorimotor, Ventral attention), and coordinating motor responses (Subcortical, Cerebellum). Prior ASD studies observed similar functional connectivity alterations between Fronto-Parietal and DMN networks, which predicted repetitive behavior symptoms (Uddin et al., 2014) and regions responding to theory-of-mind tasks and the 'mirror neuron' network (Fishman et al., 2014). These findings, together with ours, converge on the theme that functional connectivity alterations in ASD exist within networks and across networks (but see Di Martino et al., 2014). Higher cross-network interaction of the DMN in ASD, quantified as a higher participation coefficient in the present study, adds to other graph theory measures such as degree centrality (Di Martino et al., 2014) and mean global functional connectivity (Supekar et al., 2013), which also revealed greater regional interaction in ASD, but without regard to network assignment. Growing demonstrations of greater interaction across brain regions (or networks) in ASD are compatible with an emerging excitation/inhibition imbalance hypothesis of ASD. This hypothesis is rooted in evidence of genetic, receptor, and enzyme deficits in the gamma-aminobutyric acid (GABA) signaling in animal models of ASD (Rubenstein, 2011; Rubenstein and Merzenich, 2003; Yizhar et al., 2011). Diminished GABAergic function is hypothesized to disrupt the excitatory/inhibitory balance at the neuronal level, and this affects the formation and stabilization of synapses (presynaptic terminals and dendritic spines) during brain development, which in turn, leads to mostly over-connectivity and poorly segregated networks in ASD (Pizzarelli and Cherubini, 2013; Rubenstein and Merzenich, 2003). While our findings cannot directly address this hypothesis, MR spectroscopy has revealed GABA abnormalities in medial prefrontal cortex, including the ACC (Cochran et al., 2015). Future investigations that combine multimodal approaches with longitudinal designs will provide the necessary evidence to evaluate the excitation/inhibition hypothesis.

Acknowledgments

We would like to acknowledge the families and children who dedicated their time and energy for the present study. We also acknowledge the following funding sources that supported the research and the investigators: Isadore and Bertha Gudelsky Foundation; Frederick and Elizabeth Singer Foundation; the National Institute of Mental Health—award numbers K23MH086111, R01MH084961, and U54MH066417; the National Institute of Child Health and Human Development—award numbers P30HD40677 and P30HD026979 (Intellectual and Developmental Disabilities Research Center at Children's National Medical Center and Children's Hospital of Philadelphia, respectively); the National Center for Research Resources—award number M01RR020359, and the Philadelphia Foundation. A portion of these data was presented at the Annual International Meeting for Autism Research in Toronto, Canada, May, 2012. Finally, we would like to thank Rafael Oliveras-Rentas, Jennifer Sokoloff, and the Center for Functional and Magnetic Resonance Imaging at Georgetown University (Director: John VanMeter, PhD) for additional support in data collection. B.E.Y., C.J.V., W.D.G., and L.K. conceived the study. B.E.Y., J.S., K.F.J., D.N.A., and R.W. carried out clinical and imaging data collection. B.E.Y., E.M.G., and T.D.S. conducted resting state data analyses. B.E.Y. and C.J.V. drafted the manuscript, and all co-authors provided critical input. The authors have no conflicts of interest with respect to the research reported in this manuscript.

Appendix A. Supplementary data

Supplementary data to this article can be found online at http://dx.doi.org/10.1016/j.nicl.2015.07.018.

References

Ameis, S.H., Fan, J., Rockel, C., Soorya, L., Wang, A.T., Anagnostou, E., 2013. Altered cingulum bundle microstructure in autism spectrum disorder. Acta Neuropsychiatr 25 (5), 275–282. http://dx.doi.org/10.1017/neu.2013.225287727.

Assaf, M., Jagannathan, K., Calhoun, V.D., Miller, L., Stevens, M.C., Sahl, R., O'Boyle, J.G., Schultz, R.T., Pearlson, G.D., 2010. Abnormal functional connectivity of default mode sub-networks in autism spectrum disorder patients. Neuroimage 53 (1), 247–256. http://dx.doi.org/10.1016/j.neuroimage.2010.05.06720621638.

Bassett, D.S., Bullmore, E.T., 2009. Human brain networks in health and disease. Curr. Opin. Neurol. 22 (4), 340–347. http://dx.doi.org/10.1097/WCO.0b013e32832d93dd19494774.

Benjamini, Y., Hochberg, Y., 1995. Controlling the false discovery rate—a practical and powerful approach to multiple testing. J. R. Stat. Soc. B stat. methodol. 57, 289–300.

Bolling, D.Z., Pitskel, N.B., Deen, B., Crowley, M.J., McPartland, J.C., Kaiser, M.D., Vander Wyk, B.C., Wu, J., Mayes, L.C., Pelphrey, K.A., 2011. Enhanced neural responses to rule violation in children with autism: a comparison to social exclusion. Dev. Cogn. Neurosci. 1 (3), 280–294. http://dx.doi.org/10.1016/j.dcn.2011.02.00221743819.

Brett, M., Anton, J., Valabregue, R., Pioline, J., 2002. Region of interest analysis using an SPM toolbox. NeuroImage 16.

Buckner, R.L., Andrews-Hanna, J.R., Schacter, D.L., 2008. The brain's default network: anatomy, function, and relevance to disease. Ann. N. Y. Acad. Sci. 1124, 1–38. http://dx.doi.org/10.1196/annals.1440.01118400922.

Bullmore, E., Sporns, O., 2009. Complex brain networks: graph theoretical analysis of structural and functional systems. Nat. Rev. Neurosci. 10 (3), 186–198. http://dx.doi.org/10.1038/nrn257519190637.

Casanova, M.F., van Kooten, I.A.J., Switala, A.E., van Engeland, H., Heinsen, H., Steinbusch, H.W.M., Hof, P.R., Trippe, J., Stone, J., Schmitz, C., 2006. Minicolumnar abnormalities in autism. Acta Neuropathol. 112 (3), 287–303. http://dx.doi.org/10.1007/s00401-006-0085-516819561.

Castellanos, F.X., Tannock, R., 2002. Neuroscience of attention-deficit/hyperactivity disorder: the search for endophenotypes. Nat. Rev. Neurosci. 3 (8), 617–628. http://dx.doi.org/10.1038/nrn89612154363.

Castelli, F., Frith, C., Happé, F., Frith, U., 2002. Autism, Asperger syndrome and brain mechanisms for the attribution of mental states to animated shapes. Brain 125 (8), 1839–1849. http://dx.doi.org/10.1093/brain/awf18912135974.

Cauda, F., Geda, E., Sacco, K., D'Agata, F., Duca, S., Geminiani, G., Keller, R., 2011. Grey matter abnormality in autism spectrum disorder: an activation likelihood estimation meta-analysis study. J. Neurol. Neurosurg. Psychiatry 82 (12), 1304–1313. http://dx.doi.org/10.1136/jnnp.2010.23911121693631.

Cherkassky, V.L., Kana, R.K., Keller, T.A., Just, M.A., 2006. Functional connectivity in a baseline resting-state network in autism. Neuroreport 17 (16), 1687–1690. http://dx.doi.org/10.1097/01.wnr.0000239956.45448.4c17047454.

Cochran, D.M., Sikoglu, E.M., Hodge, S.M., Edden, R.A.E., Foley, A., Kennedy, D.N., Moore, C.M., Frazier, J.A., 2015. Relationship among glutamine, γ-aminobutyric acid, and social cognition in autism spectrum disorders. J. Child Adolesc. Psychopharmacol. 25 (4), 314–322. http://dx.doi.org/10.1089/cap.2014.011225919578.

Cohen, J., 1988. Statistical Power Analysis for the Behavioral Sciences. Second edition Erlbaum, Hillsdale, NJ.

Deen, B., Pelphrey, K., 2012. Perspective: brain scans need a rethink. Nature 491 (7422), S20. http://dx.doi.org/10.1038/491S20a23136657.

Di Martino, A., Yan, C.-G., Li, Q., Denio, E., Castellanos, F.X., Alaerts, K., Anderson, J.S., Assaf, M., Bookheimer, S.Y., Dapretto, M., Deen, B., Delmonte, S., Dinstein, I., Ertl-Wagner, B., Fair, D.A., Gallagher, L., Kennedy, D.P., Keown, C.L., Keysers, C., Lainhart, J.E., Lord, C., Luna, B., Menon, V., Minshew, N.J., Monk, C.S., Mueller, S., Müller, R.-A., Nebel, M.B., Nigg, J.T., O'Hearn, K., Pelphrey, K.A., Peltier, S.J., Rudie, J.D., Sunaert, S., Thioux, M., Tyszka, J.M., Uddin, L.Q., Verhoeven, J.S., Wenderoth, N., Wiggins, J.L., Mostofsky, S.H., Milham, M.P., 2014. The autism brain imaging data exchange: towards a large-scale evaluation of the intrinsic brain architecture in autism. Mol. Psychiatry http://dx.doi.org/10.1038/mp.2013.78.

Dosenbach, N.U.F., Fair, D.A., Miezin, F.M., Cohen, A.L., Wenger, K.K., Dosenbach, R.A.T., Fox, M.D., Snyder, A.Z., Vincent, J.L., Raichle, M.E., Schlaggar, B.L., Petersen, S.E., 2007. Distinct brain networks for adaptive and stable task control in humans. Proc. Natl. Acad. Sci. U. S. A. 104 (26), 11073–11078. http://dx.doi.org/10.1073/pnas.0704320104175769222.

Doyle-Thomas, K.A.R., Lee, W., Foster, N.E.V., Tryfon, A., Ouimet, T., Hyde, K.L., Evans, A.C., Lewis, J., Zwaigenbaum, L., Anagnostou, E., 2015. Atypical functional brain connectivity during rest in autism spectrum disorders. Ann. Neurol. http://dx.doi.org/10.1002/ana.2439125707715.

Duerden, E.G., Mak-Fan, K.M., Taylor, M.J., Roberts, S.W., 2012. Regional differences in grey and white matter in children and adults with autism spectrum disorders: an activation likelihood estimate (ALE) meta-analysis. Autism Res. 5 (1), 49–66. http://dx.doi.org/10.1002/aur.23522139976.

Eilam-Stock, T., Xu, P., Cao, M., Gu, X., Van Dam, N.T., Anagnostou, E., Kolevzon, A., Soorya, L., Park, Y., Siller, M., He, Y., Hof, P.R., Fan, J., 2014. Abnormal autonomic and associated brain activities during rest in autism spectrum disorder. Brain 137 (1), 153–171. http://dx.doi.org/10.1093/brain/awt29424424916.

Fair, D.A., Dosenbach, N.U.F., Church, J.A., Cohen, A.L., Brahmbhatt, S., Miezin, F.M., Barch, D.M., Raichle, M.E., Petersen, S.E., Schlaggar, B.L., 2007. Development of distinct control networks through segregation and integration. Proc. Natl. Acad. Sci. U. S. A. 104 (33), 13507–13512. http://dx.doi.org/10.1073/pnas.070584310417679691.

Fishman, I., Keown, C.L., Lincoln, A.J., Pineda, J.A., Müller, R.-A., 2014. Atypical Cross talk between mentalizing and mirror neuron networks in autism spectrum disorder. J.A.M.A. Psychiatry 71 (7), 751–760. http://dx.doi.org/10.1001/jamapsychiatry.2014.8324740586.

Fox, M.D., Zhang, D., Snyder, A.Z., Raichle, M.E., 2009. The global signal and observed anticorrelated resting state brain networks. J. Neurophysiol. 101 (6), 3270–3283. http://dx.doi.org/10.1152/jn.90777.200819339462.

Fukunaga, M., Horovitz, S.G., van Gelderen, P., de Zwart, J.A., Jansma, J.M., Ikonomidou, V.N., Chu, R., Deckers, R.H.R., Leopold, D.A., Duyn, J.H., 2006. Large-amplitude, spatially correlated fluctuations in BOLD fMRI signals during extended rest and early sleep stages. Magn. Reson. Imaging 24 (8), 979–992. http://dx.doi.org/10.1016/j.mri.2006.04.01816997067.

Gadow, K.D., Sprafkin, J., 2010. Child & Adolescent Symptom Inventory. Fourth edition revised Checkmate Plus, Stony Brook, NY.

Gordon, E.M., Lee, P.S., Maisog, J.M., Foss-Feig, J., Billington, M.E., Vanmeter, J., Vaidya, C.J., 2011. Strength of default mode resting-state connectivity relates to white matter integrity in children. Dev. Sci. 14 (4), 738–751. http://dx.doi.org/10.1111/j.1467-7687.2010.01020.x21676094.

Gotham, K., Pickles, A., Lord, C., 2009. Standardizing ADOS scores for a measure of severity in autism spectrum disorders. J. Autism Dev. Disord. 39 (5), 693–705. http://dx.doi.org/10.1007/s10803-008-0674-319082876.

Hallquist, M.N., Hwang, K., Luna, B., 2013. The nuisance of nuisance regression: spectral misspecification in a common approach to resting-state fMRI preprocessing reintroduces noise and obscures functional connectivity. Neuroimage 82, 208–225. http://dx.doi.org/10.1016/j.neuroimage.2013.05.116.

Ikuta, T., Shafritz, K.M., Bregman, J., Peters, B.D., Gruner, P., Malhotra, A.K., Szeszko, P.R., 2014. Abnormal cingulum bundle development in autism: a probabilistic tractography study. Psychiatry Res. Neuroimag. 221 (1), 63–68. http://dx.doi.org/10.1016/j.pscychresns.2013.08.00224231056.

Jiao, Y., Chen, R., Ke, X., Chu, K., Lu, Z., Herskovits, E.H., 2010. Predictive models of autism spectrum disorder based on brain regional cortical thickness. Neuroimage 50 (2), 589–599. http://dx.doi.org/10.1016/j.neuroimage.2009.12.04720026220.

Jung, M., Kosaka, H., Saito, D.N., Ishitobi, M., Morita, T., Inohara, K., Asano, M., Arai, S., Munesue, T., Tomoda, A., Wada, Y., Sadato, N., Okazawa, H., Iidaka, T., 2014. Default mode network in young male adults with autism spectrum disorder: relationship with autism spectrum traits. Mol. Autism 5, 35. http://dx.doi.org/10.1186/2040-2392-5-3524955232.

Kana, R.K., Libero, L.E., Hu, C.P., Deshpande, H.D., Colburn, J.S., 2014. Functional brain networks and white matter underlying theory-of-mind in autism. Social Cogn. Affect. Neurosci. 9 (1), 98–105. http://dx.doi.org/10.1093/scan/nss106.

Kennedy, D.P., Courchesne, E., 2008. The intrinsic functional organization of the brain is altered in autism. Neuroimage 39 (4), 1877–1885. http://dx.doi.org/10.1016/j.neuroimage.2007.10.05218083565.

Kleinhans, N.M., Richards, T., Sterling, L., Stegbauer, K.C., Mahurin, R., Johnson, L.C., Greenson, J., Dawson, G., Aylward, E., 2008. Abnormal functional connectivity in autism spectrum disorders during face processing. Brain 131 (4), 1000–1012. http://dx.doi.org/10.1093/brain/awm33418234695.

Knutson, B., Westdorp, A., Kaiser, E., Hommer, D., 2000. fMRI visualization of brain activity during a monetary incentive delay task. Neuroimage 12 (1), 20–27. http://dx.doi.org/10.1006/nimg.2000.059310875899.

Lombardo, M.V., Chakrabarti, B., Bullmore, E.T., Sadek, S.A., Pasco, G., Wheelwright, S.J., Suckling, J., MRC AIMS Consortium, Baron-Cohen, S., 2010. Atypical neural self-representation in autism. Brain 133 (2), 611–624. http://dx.doi.org/10.1093/brain/awp30620008375.

Lord, C., Risi, S., Lambrecht, L., Cook, E.H., Leventhal, B.L., DiLavore, P.C., Pickles, A., Rutter, M., 2000. The autism diagnostic observation schedule-generic: a standard measure of social and communication deficits associated with the spectrum of autism. J. Autism Dev. Disord. 30 (3), 205–22311055457.

Lord, C., Rutter, M., Le Couteur, A., 1994. Autism diagnostic interview-revised: a revised version of a diagnostic interview for caregivers of individuals with possible pervasive developmental disorders. J. Autism Dev. Disord. 24 (5), 659–6857814313.

Lynch, C.J., Uddin, L.Q., Supekar, K., Khouzam, A., Phillips, J., Menon, V., 2013. Default mode network in childhood autism: posteromedial cortex heterogeneity and relationship with social deficits. Biol. Psychiatry 74 (3), 212–219. http://dx.doi.org/10.1016/j.biopsych.2012.12.01323375976.

Marquand, A.F., De Simoni, S., O'Daly, O.G., Williams, S.C.R., Mourão-Miranda, J., Mehta, M.A., 2011. Pattern classification of working memory networks reveals differential effects of methylphenidate, atomoxetine, and placebo in healthy volunteers. Neuropsychopharmacology 36 (6), 1237–1247. http://dx.doi.org/10.1038/npp.2011.921346736.

Mason, R.A., Williams, D.L., Kana, R.K., Minshew, N., Just, M.A., 2008. Theory of mind disruption and recruitment of the right hemisphere during narrative comprehension in autism. Neuropsychologia 46 (1), 269–280. http://dx.doi.org/10.1016/j.neuropsychologia.2007.07.01817869314.

McCabe, C., Mishor, Z., 2011. Antidepressant medications reduce subcortical-cortical resting-state functional connectivity in healthy volunteers. Neuroimage 57 (4), 1317–1323. http://dx.doi.org/10.1016/j.neuroimage.2011.05.05121640839.

Monk, C.S., Peltier, S.J., Wiggins, J.L., Weng, S.-J., Carrasco, M., Risi, S., Lord, C., 2009. Abnormalities of intrinsic functional connectivity in autism spectrum disorders. Neuroimage 47 (2), 764–772. http://dx.doi.org/10.1016/j.neuroimage.2009.04.06919409498.

Müller, R.-A., Shih, P., Keehn, B., Deyoe, J.R., Leyden, K.M., Shukla, D.K., 2011. Underconnected, but how? A survey of functional connectivity MRI studies in autism spectrum disorders. Cereb. Cortex 21 (10), 2233–2243. http://dx.doi.org/10.1093/cercor/bhq29621378114.

Murdaugh, D.L., Shinkareva, S.V., Deshpande, H.R., Wang, J., Pennick, M.R., Kana, R.K., 2012. Differential deactivation during mentalizing and classification of autism based on default mode network connectivity. PLOS One 7 (11), e50064. http://dx.doi.org/10.1371/journal.pone.005006423185536.

Nair, A., Keown, C.L., Datko, M., Shih, P., Keehn, B., Müller, R.-A., 2014. Impact of methodological variables on functional connectivity findings in autism spectrum disorders. Hum. Brain Mapp. 35 (8), 4035–4048. http://dx.doi.org/10.1002/hbm.2245624452854.

O'Doherty, J.P., 2004. Reward representations and reward-related learning in the human brain: insights from neuroimaging. Curr. Opin. Neurobiol. 14 (6), 769–776. http://dx.doi.org/10.1016/j.conb.2004.10.01615582382.

Oblak, A.L., Gibbs, T.T., Blatt, G.J., 2011. Reduced GABAA receptors and benzodiazepine binding sites in the posterior cingulate cortex and fusiform gyrus in autism. Brain Res. 1380, 218–228. http://dx.doi.org/10.1016/j.brainres.2010.09.02120858465.

Oblak, A.L., Rosene, D.L., Kemper, T.L., Bauman, M.L., Blatt, G.J., 2011. Altered posterior cingulate cortical cyctoarchitecture, but normal density of neurons and interneurons in the posterior cingulate cortex and fusiform gyrus in autism. Autism Res. 4 (3), 200–211. http://dx.doi.org/10.1002/aur.18821360830.

Ou, Y., Sotiras, A., Paragios, N., Davatzikos, C., 2011. DRAMMS: deformable registration via attribute matching and mutual-saliency weighting. Medical Image Analysis, Special Section on IPMI 2009 (15), 622–639. http://dx.doi.org/10.1016/j.media.2010.07.002.

Pizzarelli, R., Cherubini, E., 2013. Developmental regulation of GABAergic signalling in the hippocampus of neuroligin 3 R451C knock-in mice: an animal model of autism. Front. Cell. Neurosci. 7, 85. http://dx.doi.org/10.3389/fncel.2013.0008523761734.

Power, J.D., Barnes, K.A., Snyder, A.Z., Schlaggar, B.L., Petersen, S.E., 2012. Spurious but systematic correlations in functional connectivity MRI networks arise from subject motion. NeuroImage 59 (3), 2142–2154. http://dx.doi.org/10.1016/j.neuroimage.2011.10.01822019881.

Power, J.D., Cohen, A.L., Nelson, S.M., Wig, G.S., Barnes, K.A., Church, J.A., Vogel, A.C., Laumann, T.O., Miezin, F.M., Schlaggar, B.L., Petersen, S.E., 2011. Functional network organization of the human brain. Neuron 72 (4), 665–678. http://dx.doi.org/10.1016/j.neuron.2011.09.00622099467.

Power, J.D., Mitra, A., Laumann, T.O., Snyder, A.Z., Schlaggar, B.L., Petersen, S.E., 2014. Methods to detect, characterize, and remove motion artifact in resting state fMRI. NeuroImage 84, 320–341. http://dx.doi.org/10.1016/j.neuroimage.2013.08.04823994314.

Raichle, M.E., MacLeod, A.M., Snyder, A.Z., Powers, W.J., Gusnard, D.A., Shulman, G.L., 2001. A default mode of brain function. Proc. Natl. Acad. Sci. U. S. A. 98 (2), 676–682.

Ray, S., Miller, M., Karalunas, S., Robertson, C., Grayson, D.S., Cary, R.P., Hawkey, E., Painter, J.G., Kriz, D., Fombonne, E., Nigg, J.T., Fair, D.A., 2014. Structural and functional connectivity of the human brain in autism spectrum disorders and attention-deficit/hyperactivity disorder: a rich club-organization study. Hum. Brain Mapp. 35 (12), 6032–6048. http://dx.doi.org/10.1002/hbm.2260325116862.

Rojas, D.C., Peterson, E., Winterrowd, E., Reite, M.L., Rogers, S.J., Tregellas, J.R., 2006. Regional gray matter volumetric changes in autism associated with social and repetitive behavior symptoms. B.M.C. Psychiatry 6, 56. http://dx.doi.org/10.1186/1471-244X-6-5617166273.

Rubenstein, J.L., 2011. Annual research review: development of the cerebral cortex: implications for neurodevelopmental disorders. J Child Psychol Psychiatry 52 (4), 339–355. http://dx.doi.org/10.1111/j.1469-7610.2010.02307.x20735793.

Rubenstein, J.L.R., Merzenich, M.M., 2003. Model of autism: increased ratio of excitation/inhibition in key neural systems. Genes Brain Behav. 2 (5), 255–267. http://dx.doi.org/10.1034/j.1601-183X.2003.00037.x14606691.

Rubinov, M., Sporns, O., 2010. Complex network measures of brain connectivity: uses and interpretations. Neuroimage 52 (3), 1059–1069. http://dx.doi.org/10.1016/j.neuroimage.2009.10.00319819337.

Rudie, J.D., Brown, J.A., Beck-Pancer, D., Hernandez, L.M., Dennis, E.L., Thompson, P.M., Bookheimer, S.Y., Dapretto, M., 2012a. Altered functional and structural brain network organization in autism. Neuroimage Clin. 2, 79–94. http://dx.doi.org/10.1016/j.nicl.2012.11.00624179761.

Rudie, J.D., Shehzad, Z., Hernandez, L.M., Colich, N.L., Bookheimer, S.Y., Iacoboni, M., Dapretto, M., 2012b. Reduced functional integration and segregation of distributed neural systems underlying social and emotional information processing in autism spectrum disorders. Cereb. Cortex 22 (5), 1025–1037. http://dx.doi.org/10.1093/cercor/bhr17121784971.

Sambataro, F., Blasi, G., Fazio, L., Caforio, G., Taurisano, P., Romano, R., Di Giorgio, A., Gelao, B., Lo Bianco, L., Papazacharias, A., Popolizio, T., Nardini, M., Bertolino, A., 2010. Treatment with olanzapine is associated with modulation of the default mode network in patients with schizophrenia. Neuropsychopharmacology 35 (4), 904–912. http://dx.doi.org/10.1038/npp.2009.19219956088.

Satterthwaite, T.D., Elliott, M.A., Gerraty, R.T., Ruparel, K., Loughead, J., Calkins, M.E., Eickhoff, S.B., Hakonarson, H., Gur, R.C., Gur, R.E., Wolf, D.H., 2013a. An improved framework for confound regression and filtering for control of motion artifact in the preprocessing of resting-state functional connectivity data. NeuroImage 64, 240–256. http://dx.doi.org/10.1016/j.neuroimage.2012.08.05222926292.

Satterthwaite, T.D., Wolf, D.H., Ruparel, K., Erus, G., Elliott, M.A., Eickhoff, S.B., Gennatas, E.D., Jackson, C., Prabhakaran, K., Smith, A., Hakonarson, H., Verma, R., Davatzikos, C., Gur, R.E., Gur, R.C., 2013b. Heterogeneous impact of motion on fundamental patterns of developmental changes in functional connectivity during youth. NeuroImage 83, 45–57. http://dx.doi.org/10.1016/j.neuroimage.2013.06.04523792981.

Satterthwaite, T.D., Wolf, D.H., Roalf, D.R., Ruparel, K., Erus, G., Vandekar, S., Gennatas, E.D., Elliott, M.A., Smith, A., Hakonarson, H., Verma, R., Davatzikos, C., Gur, R.E., Gur, R.C., 2014. Linked sex differences in cognition and functional connectivity in youth. Cereb. Cortex 36. http://dx.doi.org/10.1093/cercor/bhu03624646613.

Seeley, W.W., Menon, V., Schatzberg, A.F., Keller, J., Glover, G.H., Kenna, H., Reiss, A.L., Greicius, M.D., 2007. Dissociable intrinsic connectivity networks for salience processing and executive control. J. Neurosci. 27 (9), 2349–2356. http://dx.doi.org/10.1523/JNEUROSCI.5587-06.200717329432.

Shih, P., Keehn, B., Oram, J.K., Leyden, K.M., Keown, C.L., Müller, R.-A., 2011. Functional differentiation of posterior superior temporal sulcus in autism: a functional connectivity magnetic resonance imaging study. Biol. Psychiatry 70 (3), 270–277. http://dx.doi.org/10.1016/j.biopsych.2011.03.04021601832.

Shukla, D.K., Keehn, B., Müller, R.-A., 2011. Tract-specific analyses of diffusion tensor imaging show widespread white matter compromise in autism spectrum disorder. J. Child Psychol. Psychiatry 52 (3), 286–295. http://dx.doi.org/10.1111/j.1469-7610.2010.02342.x21073464.

Smith, S.M., Fox, P.T., Miller, K.L., Glahn, D.C., Fox, P.M., Mackay, C.E., Filippini, N., Watkins, K.E., Toro, R., Laird, A.R., Beckmann, C.F., 2009. Correspondence of the brain's functional architecture during activation and rest. Proc. Natl. Acad. Sci. U. S. A. 106 (31), 13040–13045. http://dx.doi.org/10.1073/pnas.090526710619620724.

Smith, S.M., Jenkinson, M., Woolrich, M.W., Beckmann, C.F., Behrens, T.E.J., Johansen-Berg, H., Bannister, P.R., De Luca, M., Drobnjak, I., Flitney, D.E., Niazy, R.K., Saunders, J., Vickers, J., Zhang, Y., De Stefano, N., Brady, J.M., Matthews, P.M., 2004. Advances in functional and structural MR image analysis and implementation as FSL. NeuroImage 23, S208–S219. http://dx.doi.org/10.1016/j.neuroimage.2004.07.05115501092.

Supekar, K., Uddin, L.Q., Khouzam, A., Phillips, J., Gaillard, W.D., Kenworthy, L.E., Yerys, B.E., Vaidya, C.J., Menon, V., 2013. Brain hyperconnectivity in children with autism and its links to social deficits. Cell Rep. 5 (3), 738–747. http://dx.doi.org/10.1016/j.celrep.2013.10.00124210821.

Supekar, K., Uddin, L.Q., Prater, K., Amin, H., Greicius, M.D., Menon, V., 2010. Development of functional and structural connectivity within the default mode network in young children. Neuroimage 52 (1), 290–301. http://dx.doi.org/10.1016/j.neuroimage.2010.04.00920385244.

Uddin, L.Q., Davies, M.S., Scott, A.A., Zaidel, E., Bookheimer, S.Y., Iacoboni, M., Dapretto, M., 2008. Neural basis of self and other representation in autism: an fMRI study of self-face recognition. PLOS One 3 (10), e3526. http://dx.doi.org/10.1371/journal.pone.000352618958161.

Uddin, L.Q., Menon, V., Young, C.B., Ryali, S., Chen, T., Khouzam, A., Minshew, N.J., Hardan, A.Y., 2011. Multivariate searchlight classification of structural magnetic resonance imaging in children and adolescents with autism. Biol. Psychiatry 70 (9), 833–841. http://dx.doi.org/10.1016/j.biopsych.2011.07.01421890111.

Uddin, L.Q., Supekar, K., Lynch, C.J., Cheng, K.M., Odriozola, P., Barth, M.E., Phillips, J., Feinstein, C., Abrams, D.A., Menon, V., 2014. Brain state differentiation and behavioral inflexibility in autism. Cereb. Cortex 161. http://dx.doi.org/10.1093/cercor/bhu16125073720.

Vaidya, C.J., Gordon, E.M., 2013. Phenotypic variability in resting-state functional connectivity: current status. Brain Connect. 3 (2), 99–120. http://dx.doi.org/10.1089/brain.2012.011023294010.

Van Dijk, K.R.A., Hedden, T., Venkataraman, A., Evans, K.C., Lazar, S.W., Buckner, R.L., 2010. Intrinsic functional connectivity as a tool for human connectomics: theory, properties, and optimization. J. Neurophysiol. 103 (1), 297–321. http://dx.doi.org/10.1152/jn.00783.200919889849.

Van Dijk, K.R.A., Sabuncu, M.R., Buckner, R.L., 2012. The influence of head motion on intrinsic functional connectivity MRI. NeuroImage 59 (1), 431–438. http://dx.doi.org/10.1016/j.neuroimage.2011.07.04421810475.

von dem Hagen, E.A.H., Stoyanova, R.S., Baron-Cohen, S., Calder, A.J., 2013. Reduced functional connectivity within and between "social" resting state networks in autism spectrum conditions. Soc. Cogn. affect. neurosci. 8 (6), 694–701. http://dx.doi.org/10.1093/scan/nss05322563003.

Waiter, G.D., Williams, J.H.G., Murray, A.D., Gilchrist, A., Perrett, D.I., Whiten, A., 2004. A voxel-based investigation of brain structure in male adolescents with autistic spectrum disorder. Neuroimage 22 (2), 619–625. http://dx.doi.org/10.1016/j.neuroimage.2004.02.02915193590.

Weng, S.-J., Wiggins, J.L., Peltier, S.J., Carrasco, M., Risi, S., Lord, C., Monk, C.S., 2010. Alterations of resting state functional connectivity in the default network in adolescents with autism spectrum disorders. Brain Res. 1313, 202–214. http://dx.doi.org/10.1016/j.brainres.2009.11.05720004180.

Wiggins, J.L., Peltier, S.J., Ashinoff, S., Weng, S.-J., Carrasco, M., Welsh, R.C., Lord, C., Monk, C.S., 2011. Using a self-organizing map algorithm to detect age-related changes in functional connectivity during rest in autism spectrum disorders. Brain Res. 1380, 187–197. http://dx.doi.org/10.1016/j.brainres.2010.10.10221047495.

Wilson, T.W., Franzen, J.D., Heinrichs-Graham, E., White, M.L., Knott, N.L., Wetzel, M.W., 2013. Broadband neurophysiological abnormalities in the medial prefrontal region of the default-mode network in adults with ADHD. Hum. Brain Mapp. 34 (3), 566–574. http://dx.doi.org/10.1002/hbm.2145922102400.

Yerys, B.E., Jankowski, K.F., Shook, D., Rosenberger, L.R., Barnes, K.A., Berl, M.M., Ritzl, E.K., Vanmeter, J., Vaidya, C.J., Gaillard, W.D., 2009. The fMRI success rate of children and adolescents: typical development, epilepsy, attention deficit/hyperactivity disorder, and autism spectrum disorders. Hum. Brain Mapp. 30 (10), 3426–3435. http://dx.doi.org/10.1002/hbm.2076719384887.

Yizhar, O., Fenno, L.E., Prigge, M., Schneider, F., Davidson, T.J., O'Shea, D.J., Sohal, V.S., Goshen, I., Finkelstein, J., Paz, J.T., Stehfest, K., Fudim, R., Ramakrishnan, C., Huguenard, J.R., Hegemann, P., Deisseroth, K., 2011. Neocortical excitation/inhibition balance in information processing and social dysfunction. Nature 477 (7363), 171–178. http://dx.doi.org/10.1038/nature1036021796121.

Zhang, D., Raichle, M.E., 2010. Disease and the brain's dark energy. Nat. Rev. Neurol. 6 (1), 15–28. http://dx.doi.org/10.1038/nrneurol.2009.19820057496.